Determination of the Extent of Lateral Spread and Density of Secondary Nucleation in Polymer Single Crystal Growth

Daniel Alcazar,[†,⊥] Annette Thierry,[†] Patrick Schultz,[||] Akiyoshi Kawaguchi,[‡] Stephen Z. D. Cheng,[§] and Bernard Lotz*[,†]

Institut Charles Sadron (CNRS-ULP), 6, rue Boussingault, 67083 Strasbourg, France, Institut de Génétique et de Biologie Moléculaire et Cellulaire, 1, Rue Laurent Fries, BP 163, 67404 Illkirch, France, Faculty of Science and Engineering, Ritsumeikan University, Noji-Higashi, Kusatsu, Shiga 525-8577, Japan, Maurice Morton Institute and Department of Polymer Science, The University of Akron, Akron, Ohio 44325-3909

Received July 26, 2006; Revised Manuscript Received October 16, 2006

ABSTRACT: As illustrated in an earlier work (*Macromolecules* **2006**, *39*, 1008), isotactic poly(vinylcyclohexane) (PVCH) single crystals display twinned growth sectors. Mapping of the twinned domains is possible via dark-field electron microscopy imaging. Each twinned domain results from a growth twin on the lateral growth face of the single crystal. The width of the twinned domain provides a measure of the so-called lateral spread extent, a fundamental parameter of classical theories of nucleation and growth for which only indirect estimates are available. The extent of lateral spread (and, as a corollary, the secondary nucleation density) (both average values and distribution), are determined for single crystals of PVCH produced in squalane over a wide range of crystallization temperatures (120−240 °C). These observations provide the first direct experimental data on these elementary processes in polymer crystal growth.

Introduction

Classical theories describe polymer crystal growth as the result of a secondary nucleation process, also described as a "primary surface nucleation" on an existing, flat growth face of a crystal, followed by lateral spread (Figure 1).[1] The secondary nucleation is energetically the more costly step, whereas lateral spread involves only the surface energy associated with chain folding. The width L' of the growth front covered by lateral growth is an important parameter in the theories of crystal growth. It is equal to the "niche separation" in the case of a polynucleation growth regime (regimes II or III of the Lauritzen−Hoffman theory). In the (ideal) mononucleation regime I, the whole length L of the growth face is covered via a single nucleation event. The growth rate perpendicular to the growth front, G, is, in the various "growth regimes" a product that involves the rate at which the lateral spread proceeds, g, the surface nucleation rate, i, and/or L or L', together with the thickness of the depositing layer or thickness of a stem, b (Figure 1).

The density of secondary nucleation, and, as a corollary, the extent of lateral spread L', are quantities that are difficult to assess since neither i nor g nor L' can be determined independently. Only estimates of the lateral spread are available, or indirect evaluations that rest on different experimental evidences.

Only the total flux, that is, the crystal growth rate G, is measurable. It has been used as a (indirect) means to evaluate the extent of lateral spread. In a set of enlightening experiments, Point et al.[2] checked to see if the growth rate G depends on the width of the growth face (it should vary when the width is smaller than the lateral spread). Using a so-called isohypse technique (well-controlled temperature jumps during growth leading to isochronous decoration), these authors determined that the growth rate of polyethylene single crystals is constant, down to growth faces widths of less than 1 μm. They concluded that lateral spread must be smaller than 1 μm. As summarized in one of the latest publications of John Hoffman and in a recent review on the Hoffman−Lauritzen theory,[3] "currently, it is considered (but, we underline, not established) that the values (of the lateral spread) should be several hundred nanometers, which corresponds to the crystallite size measured via WAXD experiments".[4]

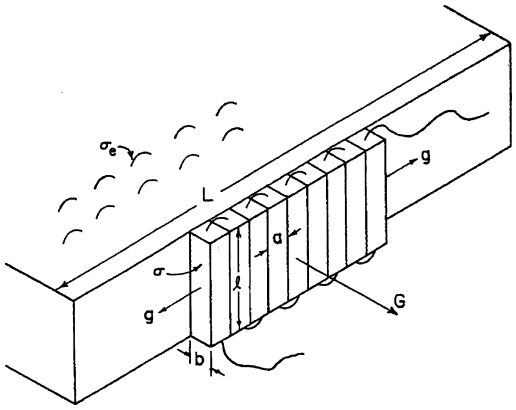

Figure 1. Classical picture of nucleation and growth on the lateral growth faces of a polymer crystal, according to Hoffman and Lauritzen. The various processes and associated rates are indicated.

The absence of any direct measure of the extent of lateral spread and density of secondary nucleation stems from the fact that, once a chain deposits on the growth face, it becomes indistinguishable from the rest of the chains. Thus, the different secondary nucleation events lose their identity and individuality since they "merge" or "blend" into the final crystal. To

* Corresponding author. E-mail: lotz@ics.u-strasbg.fr.
† Institut Charles Sadron (CNRS − ULP).
|| Institut de Génétique et de Biologie Moléculaire et Cellulaire.
‡ Faculty of Science and Engineering, Ritsumeikan University.
§ Maurice Morton Institute and Department of Polymer Science, The University of Akron.
⊥ Present address: Department of Materials Science and Engineering, Massachusetts Institute of Technology, 77 Massachusetts Avenue, Cambridge, MA 02139−4307(USA).

10.1021/ma061697x CCC: $33.50
Published on Web 12/06/2006

decompose the global growth mechanism into its more elementary processes, some kind of structural marker or another "tag" should be designed. It should highlight each individual secondary nucleation event and its associated lateral spread, or it should allow, at least, some meaningful sampling of the lateral spread.

For the majority of polymers, such a structural marker does not exist. There is no internal characteristic that enables the differentiation of a group of stems from the rest of the crystal. However, as illustrated in an earlier work from this laboratory,[5] something approaching such a marker has become available, admittedly for a specific polymer. It stems from the structural analysis of isotactic poly(vinylcyclohexane) (PVCH) that builds up crystals with two differentiable populations of stems.

In PVCH crystals, secondary nucleation and lateral spread can take place with the depositing stems either in crystallographic register with the substrate *or* in twinned relationship (the twinned domains differ by the azimuthal setting of the chains on their axis). The twinned orientation initially generated by twinned secondary nucleation spreads laterally over some length of the growth face: the inner boundary of the twinned domain is parallel to the growth front, and its width corresponds to the extent of lateral spread. Furthermore, the width and the twinned orientation of the domain are maintained during subsequent deposition of new layers, usually up to completion of the crystal. As a result of this growth twin and subsequent preservation of the twinned orientation, the four different growth sectors of PVCH single crystals are actually made of narrow, elongated microsectors perpendicular to the four different growth faces—the single crystals are polysynthetic twins. Dark field electron microscopy imaging makes it possible to map all the twinned components of the PVCH single crystals, and thus to determine the width of the twinned domains. Given the low density of twinned domains, their width is a direct measure of the lateral spread from a single secondary nucleation and provides the "sampling" referred to above.

In the present contribution, we determine the extent of lateral spread and secondary nucleation density by measuring the lateral size of the twinned microdomains formed during growth of PVCH single crystals in squalane over a wide range of crystallization temperatures (120−240 °C). This range is limited on the low-temperature side by the high density of nucleation events (i.e., by the narrowness of the twinned domains, which makes measurements difficult) and on the high-temperature side by the reduced frequency of twinning. Despite its intrinsic limitation (because twinning introduces by necessity an energy penalty relative to "normal" or untwinned growth) this study provides, to our knowledge, the first set of data in polymer crystallization that illustrates (in its literal sense also) the variation of secondary nucleation density and extent of lateral spread, both average and distribution, with crystallization temperature.

Experimental Section

The sample of PVCH was produced by Sumitomo Chemical Co (Japan). It is rather polydisperse, with number and weight-average molecular weights of $M_n = 6.7 \times 10^3$ and $M_w = 8.2 \times 10^4$, respectively (polymolecularity index: 12).

The preparation methods were essentially similar to those already described in the earlier report.[5] PVCH was dissolved in boiling squalane ($c \approx 0.05\%$ w/v) and crystallized isothermally at various crystallization temperatures (T_c). Drops of the suspension of crystals were deposited directly on carbon coated electron microscope grids. The rather "oily" squalane was washed away with heptane. Observation and selection of suitable samples for electron microscopy was performed under phase contrast with Leitz and Zeiss optical microscopes. Transmission electron microscopy (TEM) was performed with a Philips CM12 operated at 120 kV using low dose conditions required by the beam sensitivity of the material. The grid was systematically scanned at low magnification (<1000) by defocusing the diffraction pattern. Bright field images and dark fields (direct magnification of 3000) were recorded on photographic plates (Kodak SO163, developed with undiluted D19 for 12 min). Selected plates were scanned and the contrast digitally enhanced to highlight the twinned domains. Atomic force microscopy (AFM) was performed with a multimode apparatus—NanoScope IIIa controller (Digital Instruments). Drops of squalane suspension were deposited on freshly cleaved mica substrates and crystals were washed with heptane. Images were obtained in tapping mode with a tip (NanoWorld) at 320 kHz of resonance frequency and 42 N/m of force constant. High-resolution TEM was carried in a Tecnai F20 G2 (FEI, Eindhoven, The Netherlands) operating at 200 kV and equipped with a field emission gun. Images were recorded under low dose conditions (less than 20 e^-/A^2) at a magnification of 40 000× on SO163 photographic plates or on a Pelletier cooled 2K CCD camera (Ultrascan 1000, Gatan, Pleasanton). Detailed description of the analysis of high-resolution images is provided as Supporting Information.

The statistical analysis of the twinned domain width was based on 250 measurements for each T_c and was performed on printed enlargements of the dark field images. To avoid counting domains that might have formed during quenching to the selected T_c, measurements were made on the "younger" parts of the growth faces, located near the growth sector boundaries, as illustrated in Figure 7a (cf. later). Conversion of the lateral spread into number of stems is easy: since the span of one stem is 1.1 nm, the measure in nanometers corresponds within 10% to the number of stems involved in the twinned strip.

Background: Crystallography of PVCH Twins and Nucleation and Growth Processes

Crystallography and Growth Twins in PVCH Single Crystals. The stable crystal modification (form I) of PVCH has a tetragonal unit cell with parameters $a = b = 21.99$ Å, $c = 6.43$ Å, and space group $I4_1/a$.[6] (Another modification exists, with 24 residues in 7 turns of the helix[7]). The unit cell contains four helices with 4-fold symmetry: two right-handed 4_1 and two left-handed 4_3 helices. The $I4_1/a$ symmetry is characterized by the fact (fundamental in the frame of the present investigation) that, in the *c* axis projection, the helices are oriented some 17° away from the cell edges in either a clockwise or a counterclockwise rotation (hereafter referred to as cw and ccw, respectively) (Figure 2a).

The possibility of cw or ccw rotation of helices in the unit cell is at the root of a twinning by merohedry.[5] Single crystals are often twins, with twin components differing by the azimuthal setting of the chains (i.e., cw or ccw) (Figure 2a). The twinned components can be differentiated in dark-field electron microscopy, by taking advantage of the asymmetry (or "handedness") of the diffraction pattern. Strong reflections of the cw and weak reflections of the ccw parts overlap. Dark field imaging using such overlapped reflections thus reveals brighter and darker areas and allows a complete mapping of the twinned domains (Figure 3b), whereas "conventional" bright field imaging (Figure 3a) gives no clue of the underlying structural complexity of the single crystals. These different domains are represented as gray and white in the drawing of Figure 2b, to match the dark field imaging perception. The crystal lattices of the twinned components are shifted across the twin plane by one-quarter of a unit cell edge, or half the span of a single helix (Figure 2a, middle, and Figure 2b and cf., later, Figure 4).

Processes and Growth Features Involved in the Formation and Development of Growth Twins of PVCH. Figure 2b

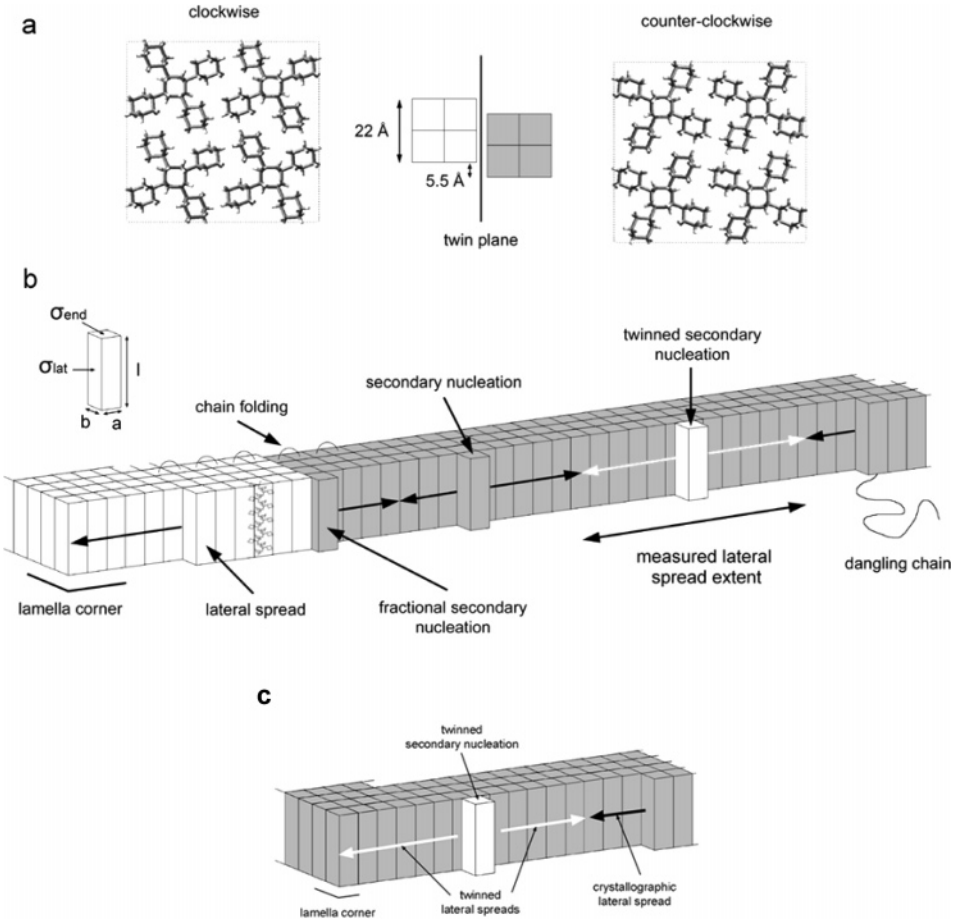

Figure 2. Crystal structure of PVCH form I, as determined by De Rosa[6] (a). The cell contains two right-handed and two left-handed helices, space group $I4_1/a$. The setting of helices is either clockwise or counterclockwise, thus giving rise to a possibility of twinning by merohedry. The twinned components are represented as light and dark (gray), to mimic their appearance in the dark field images. The center drawing illustrates the shift of helices across the twin plane, as established via an analysis of the streaks of the diffraction pattern[5] (b). The deposition process and resulting structure of the crystals examined in the present work. Twinned components are again shown as light and dark (gray). On the right of the diagram, is shown twinned secondary nucleation: deposition of a stem in twinned relationship with the substrate. It is shifted by half a stem span relative to the substrate, and has a different azimuthal setting (thus the different, white "color"). The corresponding lateral spread (white arrows) generates a twinned, "white" domain, the width of which is limited by encounter with other lateral spreads initiated by untwinned secondary nucleation (gray stems). Twin planes are soon generated that are oriented normal to the growth front (left-hand side of the drawing, frontier between gray and white domains). At the twin plane, the lattices are shifted by half a stem span in a direction normal to the growth front. This shift generates a preferred nucleation site at the jag in the growth front that corresponds to "fractional secondary nucleation" (cf. ref 5). The present work is mainly concerned with the twinned secondary nucleation and extent of associated lateral spread shown by the white arrows on the right side of the figure. The scenario of twinned secondary nucleation near a growth sector boundary leading to twinned domains in adjacent growth faces (c). When the lateral spread of the twinned layer reaches the nearby sector boundary, the twin plane is oriented normal to the growth front of that growth sector, generating a stable site for fractional secondary nucleation on that face.

illustrates the major growth processes and resulting features of PVCH crystals.

Secondary nucleation (conventional, untwinned) corresponds to the deposition of a stem in crystallographic register with the substrate (thus yielding the same gray shading). The associated lateral spread is illustrated by black arrows.

Twinned secondary nucleation corresponds to deposition of a stem (white) halfway between the substrate stems (shift of half the span of a helix). It generates, through lateral spread (white arrows), a twin plane parallel to the growth front, the extent of which is limited by the encounter with the lateral spread associated with the two neighbor secondary nucleation sites. This twin boundary will be the major concern in the present investigation: it is a growth twin boundary.

During further growth, and since the frequency of twinning is small, deposition of new stems in successive layers is in crystallographic register with the layer just formed. The initial "white" strip (arrows) in Figure 2b generates a twinned sector, which results ultimately in the elongated domains normal to the growth face observed in Figure 3.

The twinned domains are bounded by twin planes that elongate during crystal growth. Although they are the most prominent twin planes in the final crystal, they are only a consequence of the initial growth twin parallel to the growth front described above. These twin planes display also the shift of crystal lattices of half a stem width relative to their untwinned neighbor domains, i.e., along the twin boundaries normal to the growth front. The mechanism by which this shift is introduced during the growth process is not known. It amounts to a local point dislocation with a Burgers vector of $a/4$. The shift is illustrated at the boundary between white and gray domains on the left of Figure 2b, which could correspond to the boundary of a strip generated by an earlier growth twin. These twin boundaries oriented normal to the growth front feature prominently in the growth process. Indeed, the associated jag in the growth face creates a favorable deposition site, intermediate between secondary nucleation and lateral spread. It was described in an earlier report as "fractional secondary nucleation" (Figure 2b, left).

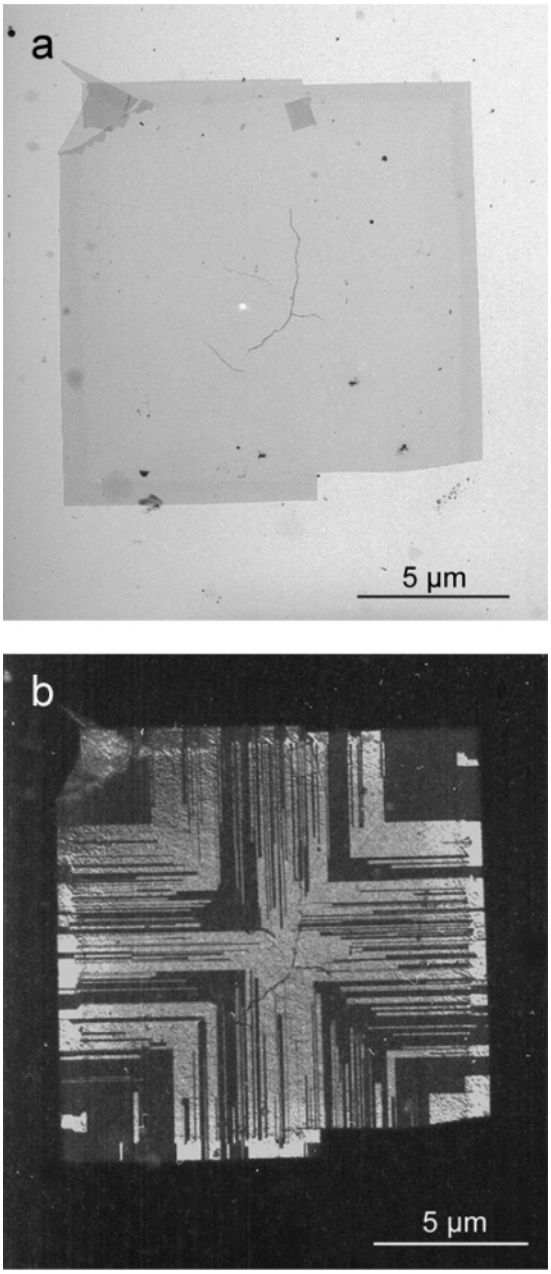

Figure 3. Bright field transmission electron micrograph of a single crystal of PVCH produced in dilute solution in squalane at 220°C. The crystal appears to be featureless (a). Dark field transmission electron micrograph of the same crystal, imaged through the overlapping 240_{cw} and 240_{ccw} diffraction spots (b). The complex mosaic of twinned domains can only be revealed by this imaging mode. Note the parallelism of the inner boundary of the twinned domains with the outer growth face, which indicates that the inner side of the twinned domains corresponds to the lateral spread after initial twinned secondary nucleation (white arrows in Figure 2b).

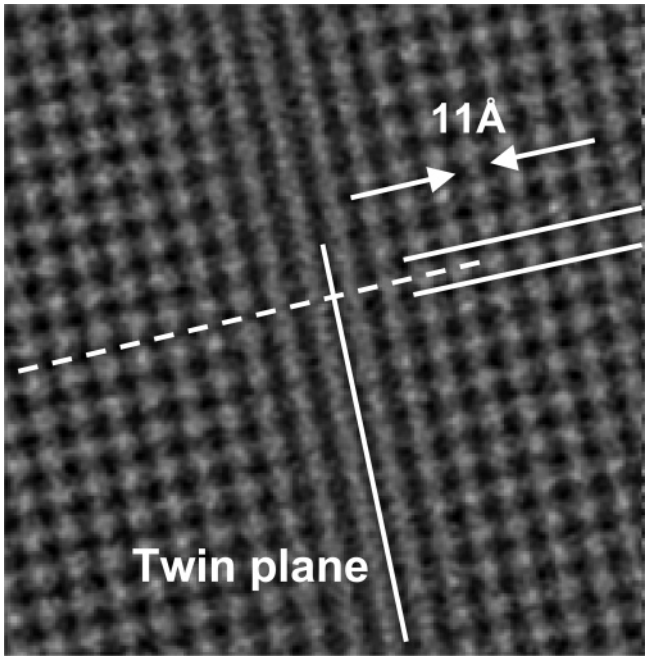

Figure 4. Noise-free image of a high-resolution electron micrograph showing a twin boundary in PVCH single crystals. The twin boundary is oriented at 11 o'clock. Crystallographic planes are underlined on both sides of the twin plane to help visualize the *a*/4 or half a stem width shift of the lattices normal to the twin boundary. Technical details of data acquisition and processing that led to this figure are provided in the Supporting Information.

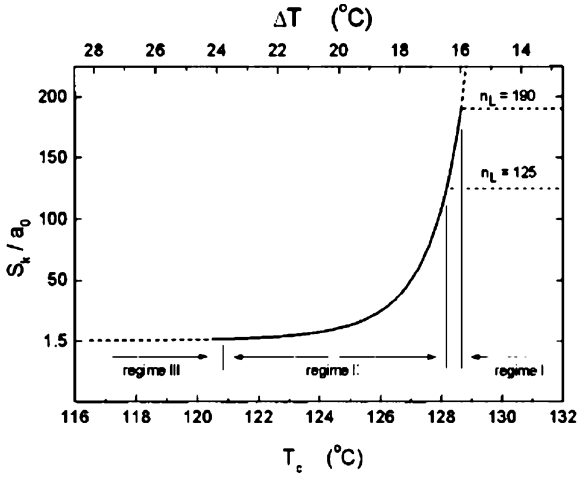

Figure 5. Diagram showing the variation of the number of stems involved in lateral spread as a function of crystallization temperature (or undercooling ΔT) for polyethylene, according to Armistead and Hoffman.[8] Note that the lateral spread shows no singularity at the transition points between different growth regimes, although the transitions are located in the asymptotic parts of the curve. Reproduced from ref 8. Copyright 2002 American Chemical Society.

Two features regarding the twin planes normal to the growth front and not previously discussed are worth reporting at this stage. *First*, we have attempted to image the twin boundary by high-resolution electron microscopy. The resolution of the images is insufficient to reveal the clockwise or counterclockwise rotation across the twin planes. However, the images reveal the shift of half a stem width just mentioned (Figure 4 and cf. Supporting Information for the details of the analysis). *Second*, in Figure 3 and others, many twin planes seem to "take the corner" near the growth sector boundaries. When a growth twin is nucleated near (but not necessarily at) the edge of the growth face, lateral spread may extend up to the lamella corner (Figure 2c). In this case, the twinned growth strip developing on one growth face generates immediately, without any further adjustment, a shift of half a stem width in the growth front of the neighbor growth face.

To summarize, and as illustrated in Figure 2b, PVCH growth involves events additional to those analyzed so far for conventional crystal growth. As discussed later, they involve different energy barriers. Assuming that the lateral energy of a twinned interface is (if only slightly) larger than that of the crystallographic packing, the three nucleation and two lateral growth events illustrated in Figure 2b may be ranked according to their decreasing energies as follows:

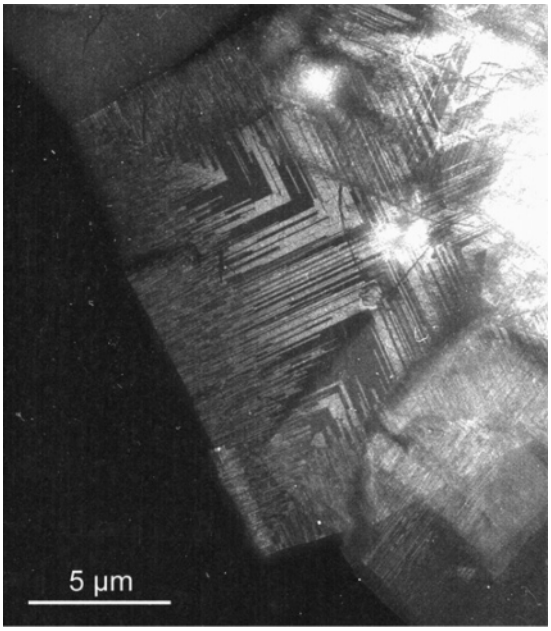

Figure 6. Single crystal of PVCH produced from a squalane solution by a moderate quench to 100 °C and imaged in dark field electron microscopy. Note the increased density of twinned domains in the exterior part of the crystal produced at lower T_c.

Twinned secondary nucleation > Secondary nucleation (crystallographic) > Fractional secondary nucleation > Twinned lateral spread > Lateral spread

Lateral Spread and Secondary Nucleation in Polymer Crystals. A major problem in assessing the validity of crystallization theories arises from the difficulty to distinguish the contribution of secondary nucleation from that of lateral spread. A given flux (global growth rate G, measurable) may be the sum of many small events (many nucleation events associated with limited lateral growth) or of fewer, more sizable events (few nucleation events that spread more on the growth face). Armistead and Hoffman[8] provide a curve, reproduced in Figure 5, showing the (assumed) variation of lateral spread vs crystallization temperature for polyethylene grown in the bulk (the ratio S_k/a_0 corresponds to the average number of stems between nucleation sites on the growth front, i.e., is the ratio of lateral spread and secondary nucleation rates). They indicate a regime III−II transition for the average niche separation (1.5 stems) determined for this regime by Guttman and Di Marzio.[9] The regime II−I transition is less clear and has been assumed to correspond to an undercooling of 16°C. The number of stems involved is, roughly speaking, above 100. As a result, and quite surprisingly, the so-called regime II extends over a very wide range of lateral spreads, from 1.5 to ≈120, i.e., a ratio of nearly 100. The main feature of interest in the context of the present work is however that *the curve is smooth*, indicating that the different growth regimes and their transitions are not determined by the extent of lateral spread (except for the onset of regime III for which it may be considered as a defining feature).

Experimental Results and Analysis

The present investigation was triggered by the experimental result illustrated in Figure 6. It displays a single crystal of PVCH produced from a squalane solution cooled by moderate quenching to 100 °C. The crystal displays a striking variation of the pattern of twinned domains from the interior to the exterior—from higher to lower crystallization temperatures. This variation has been investigated more systematically by resorting to

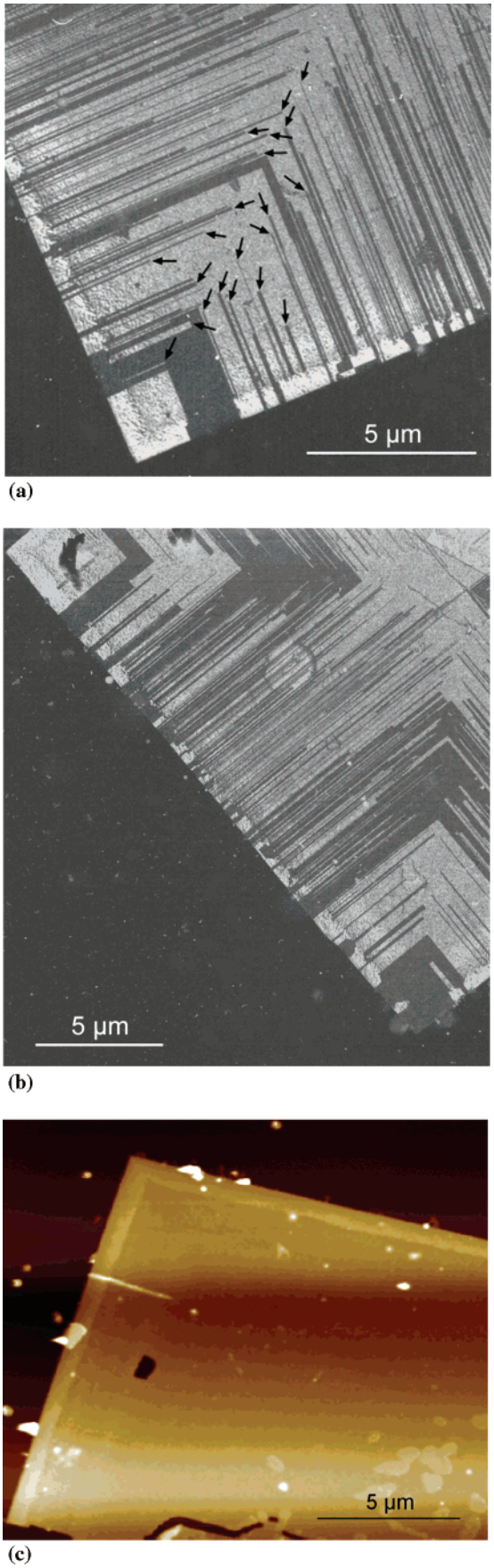

Figure 7. Dark fields (a, b) and height image by atomic force microscopy in tapping mode (c) of single crystals of PVCH produced at 220 °C.

isothermal crystallization over a wide range of temperatures. It is convenient to describe first results obtained at $T_c = 220$ °C

and at the same time to detail the experimental and interpretive procedure used throughout this work. Decreasing T_cs down to 120 °C are then considered. Crystallization at 240 °C reveals original features that require a specific development.

Crystallization at 220 °C. A single crystal produced at 220 °C is represented in Figure 7a (cf. also Figure 3). These crystals are all polysynthetic growth twins. As growth proceeds from the crystal center, growth twins develop sporadically on the growth faces: dark domains appear in lighter areas, and reciprocally. Every growth twin generates a twinned microsector with its initial edge parallel and its lateral edges normal to the growth face of the corresponding crystal sector. Since generation of twinned growth microsectors is sporadic, their density increases with the elapsed time of crystallization. As a consequence, the final density of twinned microsectors is higher near the center of the sector growth face than near its outer parts (Figure 7b for a most illustrative example). The latter areas, located near the growth sector boundaries, correspond to the "youngest" and least twinned parts of the crystal. Measurement of the width of twinned domains (arrows in Figure 7a) is made only in these freshly formed areas that are "unspoiled" by possible undesirable effects (e.g., fractional secondary nucleation associated with a nearby twin plane).

The crystal displays, besides the presence of twinned microsectors in the crystal interior, an outer, brighter rim, when imaged in dark field with the proper reflection. The rim is thicker (≈16.5 nm) than the crystal interior (≈15 nm), as attested also by AFM (Figure 7c). The rim is observed in all crystals grown in the high T_c range and therefore could well correspond to the crystallization of a low molecular weight tail of the sample. This rim has several specific characteristics. First, it frequently does not maintain the twinned orientations of the domains on which it grows: in many cases, the substrate orientation is lost, as attested by the change in brightness. Second, the inner edge of the rim forms an angle with respect to the outer crystal edge. The outer overgrowth "flattens" the crystal edges formed during the initial crystallization of the higher molecular weight fraction. As a result of sporadic nucleation of twinned microsectors, the density of twin planes abutting near the middle of the growth face is higher than that on its edges (Figure 7b). These twin planes are the sites of fractional secondary nucleation (cf. Figure 2b, left part), a preferred nucleation process that results in a faster *local* growth rate (more illustrative examples will be provided for crystals grown at $T_c = 240$ °C). As a result, the middle of the growth face "bumps out" more than the corners of the crystal. This *local* faster growth rate is highlighted by the low molecular weight crystallization—it is best perceived when looking along the growth faces in Figure 7a and b at grazing incidence.

Crystallization in the Lower T_c Range: from 200 down to 120 °C. Crystallization at lower T_cs (from 200 to 120 °C, at 20 °C intervals) shows a continuous trend. Only two representative examples ($T_c = 180$ °C, Figure 8, and 140 °C, Figure 9) are illustrated, with additional examples provided as Supporting Information.

As a rule, the density of twinned domains increases and the domain width decreases. The higher frequency of twinned nucleation results in a more sharply delineated growth sector boundary in dark field imaging, with a correlative difficulty to measure domains widths. This limits experimentally the temperature range that can be explored by this technique. At 140 and at 120 °C, the crystals break on sedimentation, indicating that they are pyramidal. Note also that the breaks are mostly and neatly normal to the growth front, parallel to the lateral twin boundaries (Figure 9b), and that the AFM images cannot reveal the very complex structure of these crystals

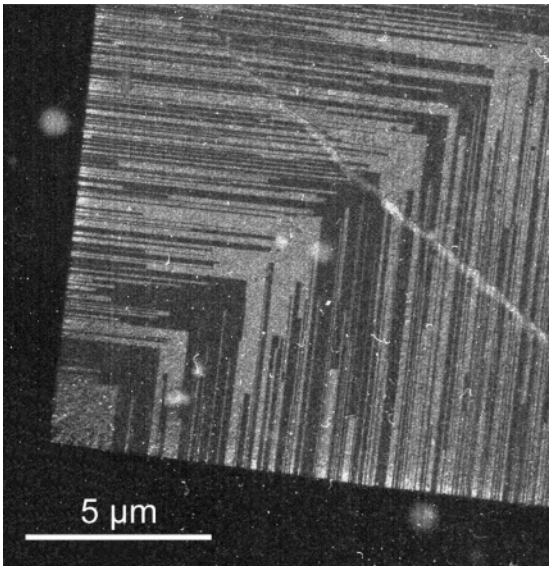

Figure 8. Dark field transmission electron micrograph of part of a single crystal of PVCH produced in squalane at 180 °C.

Analysis of the Twinned Microsector Widths. The measured twinned sector widths are displayed for each T_c (120 °C ≤ T_c ≤ 220 °C) in Figure 10. The various diagrams convey the same feeling as the micrographs: the width of the twinned domains (and therefore of lateral spread) decreases with decreasing T_c. These data are summarized after a Gaussian curve fitting procedure in Figure 11. It illustrates again the progressive narrowing of the width distribution as well as the decrease of the twin domain size as T_c decreases. Lateral spreads range from 10 to 100 nm at 120 °C and from 15 to 240 nm at 220 °C. The average lateral spread decreases, and its variation with T_c appears to slow for low T_cs. At 120 and 220 °C, the average lateral spread is 35 and 60 nm, which corresponds to average densities of secondary nucleation of 30 and 15 per micrometer for each layer of the growth face, respectively.

The smallest domain widths measured are 10 nm. This limit may be linked with the resolution of the dark field imaging technique. It may however also be a feature associated with the nature of the "probe" (twinning) used in this study. When too narrow, the twinned domain may become unstable because of the need to generate higher energy twin boundaries. Indeed, the initial growth twin results from a half stem shift parallel to the growth front but becomes stable only if during further growth it generates two twin planes with shifts normal to that growth face (corresponding to sites of fractional secondary nucleation, cf. Figure 2b). Exceedingly narrow twinned domains may thus "heal" and revert to untwinned.

Crystals Grown at $T_c = 240$ °C. Crystals produced at 240 °C (Figure 12) display a number of additional features, some of which stem from vagaries of the experimental procedure, but are very telling about the nucleation and growth processes. As a rule, the crystals display the thicker rim already observed at lower T_cs. As a rule also, the crystals produced at 240 °C display significantly less twinned domains than at lower T_cs. As a result, it is not possible to establish a viable statistic of the twinned domains widths similar to those shown in Figure 10. The widths of the few twinned domains observed in Figure 12a,b (12, 26, 42, and 75 nm) are however in the same range as for $T_c = 220$ °C.

Most of the crystals produced at 240 °C are square. Quite surprisingly, however, many of them are rectangular. Two most

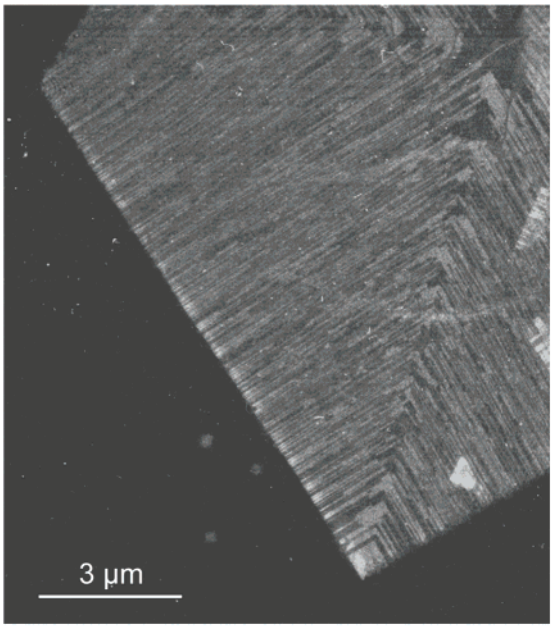

(a)

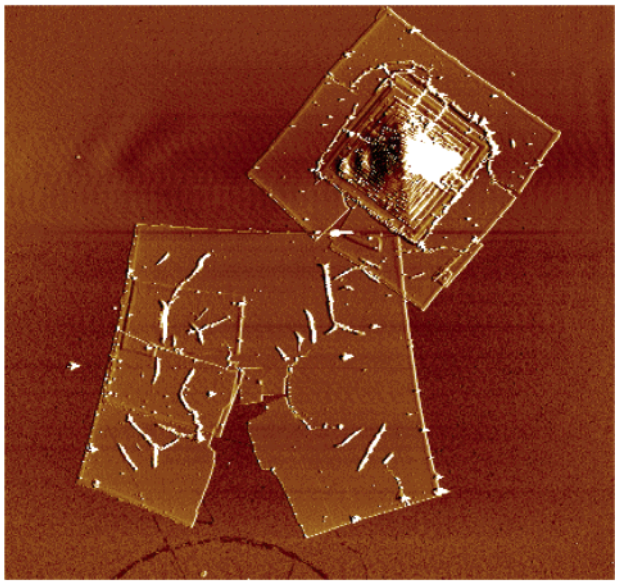

(b)

Figure 9. Dark field of part of a single crystal of PVCH produced in squalane at 140 °C (a) and height AFM image of (a) single crystals obtained under the same conditions (b).

informative crystals are shown in Figure 12. It appears that in this experiment, some form of self-seeding took place during (probably insufficient) dissolution prior to crystallization at 240 °C. The seeds are fragments of crystals produced at a lower temperature, and contain several parallel twin planes. These twin planes are maintained during growth at 240 °C, as illustrated in the enlargement of Figure 12b. The crystals are systematically elongated in the direction parallel to the twin plane that crosses the crystal center, thus owe their rectangular shape to the existence of one or several nearby twin planes in the crystal's seed. The crystal shape is determined by the higher nucleation rate associated with the abutting twin plane (fractional secondary nucleation), the lower rate of secondary nucleation on the lateral faces (thus the rectangular shape), and the virtual absence of twinned secondary nucleation. When twinning takes place (as a rule, nearly *always* in the elongated lateral growth faces), the growth rate of the corresponding face increases (cf. Figure 12a,b). Growth rate appears to be further enhanced when the abutting twin planes are associated in "bundles", i.e., are next to each other, as is the case in Figure 12b. By comparison, the crystal in Figure 12a is noticeably less elongated. The enhanced growth rate suggests a synergistic effect arising from the neighborhood of nucleation sites, possibly linked with the existence of dangling chain ends near the twin planes, as has been invoked for nucleation in regime II by Sanchez and Di Marzio.[10]

Crystals produced at 240 °C display also a thicker rim on their edges. This thicker rim helps highlight the faster growth rate associated with the twin planes in the inner part of the crystal. Indeed, the *inner edge* of the rim makes on obtuse angle ψ ($\approx$175°) centered on the abutting twin planes in the top and bottom growth faces in Figure 12b. The growth face deformation reveals the local faster nucleation process (To the contrary, the lateral faces are straight and the width of the rim is constant). The deformation of the crystal front (the 175° angle) helps evaluate the relative rates between fractional secondary nucleation and lateral spread. This ratio is simply given by $\mathrm{tg}(\psi/2) = 23$. Since the unit cell is tetragonal, the angle at the advancing front simply tells that, on average, 23 chains are deposited on the growth face by lateral spread during the time interval one new layer is formed.

Finally, it is worth pointing out that *no* twinned domains are generated on the shorter side of the rectangular crystals: the flat "steps" on the tapering growth face appear to be too small (they are 23 stems wide) for twinned nucleation to take place or to generate a "stable" twinned domain.

Atomic Force Microscopy Observations and Lamellar Thickness. The crystal thickness was estimated by AFM for some selected preparations. Figures 7c, 9b, and 12c illustrate crystals produced at 220, 140, and 240 °C, respectively. In the latter image, the thicker outer rim appears very prominently, but also the growth sector boundaries and even, slightly darker (i.e., thinner in this height mode imaging), the twin plane (or cluster of twin planes) giving rise to the overall rectangular crystal shape (at $\approx$2 o'clock from the crystal center). At 240 °C, the lamellar thickness is typically in the 13−16 nm range, with the outer rim being from 2 to up to 5 nm thicker than the crystal interior.

The thickness values are of interest when evaluated in terms of molecular length. The vinylcyclohexene monomer has a MW of 110; one turn of the helix with 0.65 nm *c* axis periodicity includes four monomers. The MW of a stem 15 nm long is thus $110 \times 4 \times (15/0.65)$, i.e., $\approx$ 10 000. The number-average MW is, given the high polymolecularity of our material ($\approx$12) only 6000. In other words, the PVCH molecules crystallize with only a rather limited number of stems per chain. For the lower MW tail of the distribution, corresponding most probably with the outer rim observed in most crystals, they could even correspond to single stems. In the inner parts of the crystals that have been our main concern during this study, the growth strips produced by secondary nucleation and lateral spread are several tens of nanometers long; i.e., they involve several tens of stems. They are therefore clearly polymolecular.

Discussion

It is convenient to examine first the possibilities and limitations of the experimental procedure used in this investigation before discussing the results in the frame of theories of nucleation and growth.

Molecular and Structural Markers Used To Analyze the Details of Polymer Crystallization. Analysis of growth

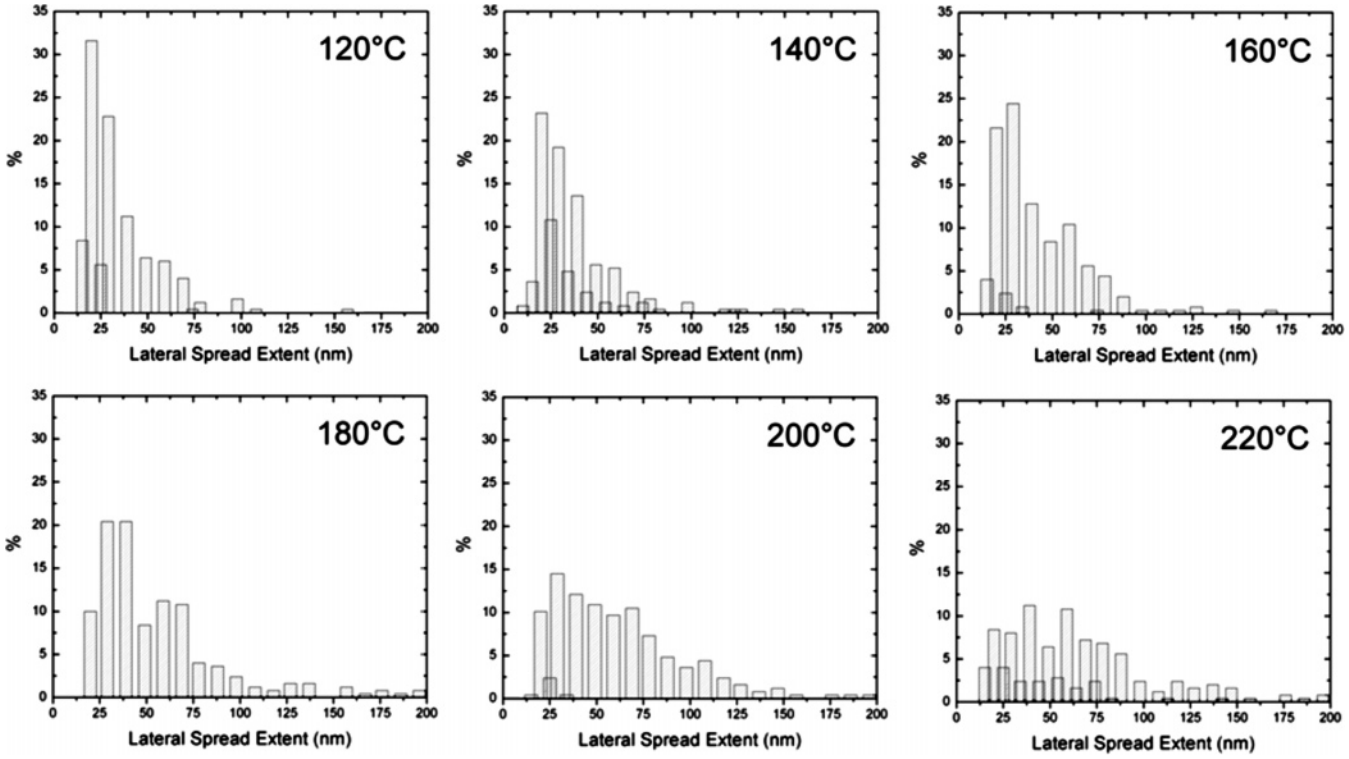

Figure 10. Width of twinned domains observed in the crystals obtained in the range 120−220 °C. 250 measurements are made at each crystallization temperature. (For easier legibility, the bars are slightly larger than the dimension interval to which they correspond, sometimes giving the feeling of overlapped distributions).

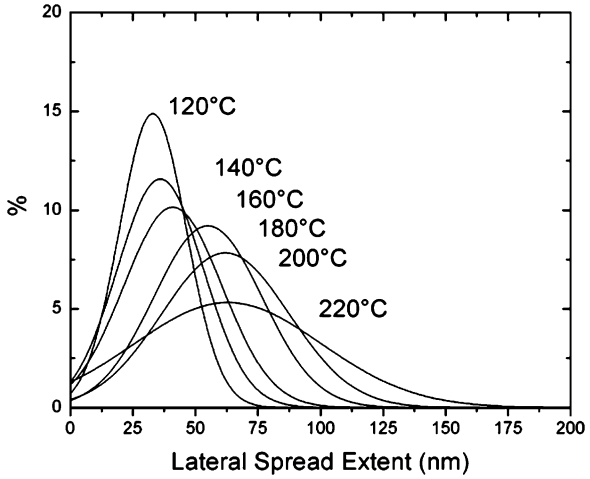

Figure 11. Variation of the twinned domains width as a function of crystallization temperature (indicated). This plot summarizes the data reported in Figure 10 after a Gaussian curve fitting procedure. Note the shift to wider domain widths when T_c increases, together with a broadening of the corresponding curves. Since the stem width is 1.1 nm, the domain width corresponds within 10% to the number of stems deposited on the growth face by lateral spread.

processes has always been a challenging task due to the difficulty or the impossibility to decompose the overall process in its elementary steps—in the present case secondary nucleation and lateral spread. As a rule, molecular and structural markers that enable analysis of the internal structure of polymer crystals at a local scale are not appropriate to evaluate lateral spread. Deuteration of part of the molecules and investigation by neutron scattering of blends with hydrogenated molecules has been used in the past. However, deuteration is suitable only when investigating the conformation and the spatial distribution of stems belonging to a single molecule. It helped establish that, in the single crystals of isotactic polystyrene,[11] the deuterated molecules are clustered in strips of stems that may extend over (e.g.) two consecutive growth layers but are also intermingled with hydrogenated stems. Polymer decoration (by fragmentation, vaporization, condensation and crystallization of polyethylene under vacuum) of the surface of polymer single crystals is only sensitive to the orientation of the folds.[12] The oriented crystallization of polymer decoration suggests that growth of single crystals results from the addition of stems in strips more or less parallel to the growth front. However, it differentiates neither the various growth strips nor the components (molecules) belonging to any one strip.

Growth twins (as opposed to the more common twinned crystals developing from a twinned seed) have been investigated in the past, but usually in a different context. Pradère et al.[13] investigated twins of isotactic poly(4-methylpentene-1) form III that rest on the same unit cell symmetry as PVCH. Their investigation was however limited to a relatively high T_c range, corresponding roughly to the situation described here for T_c = 240 °C. They did not therefore observe the systematic variation of lateral spread widths reported in the present investigation. Tsuji and collaborators investigated multiple, polysynthetic twins of the β form of syndiotactic polystyrene (sPS).[14] Various growth conditions were investigated: thin film growth at high T_c, solution crystallization. The twinned domain width was determined mainly by analysis of the streaked diffraction pattern, supplemented occasionally by dark field and by high-resolution imaging techniques. Bright fields, taken at a direct magnification of 40000×, reveal the setting of each chain in the twinned crystal—a major technical achievement, made possible (but only in part!) by the beam resistance of sPS. The width of the twinned domains in sPS is significantly smaller than for PVCH and may be down to three or four stems. Also, the crystallography (unit cell symmetry) is less favorable than for PVCH. Twinning in sPS was thus analyzed (correctly, but only) in the frame of multiple twinning or structural disorder and not, as is possible

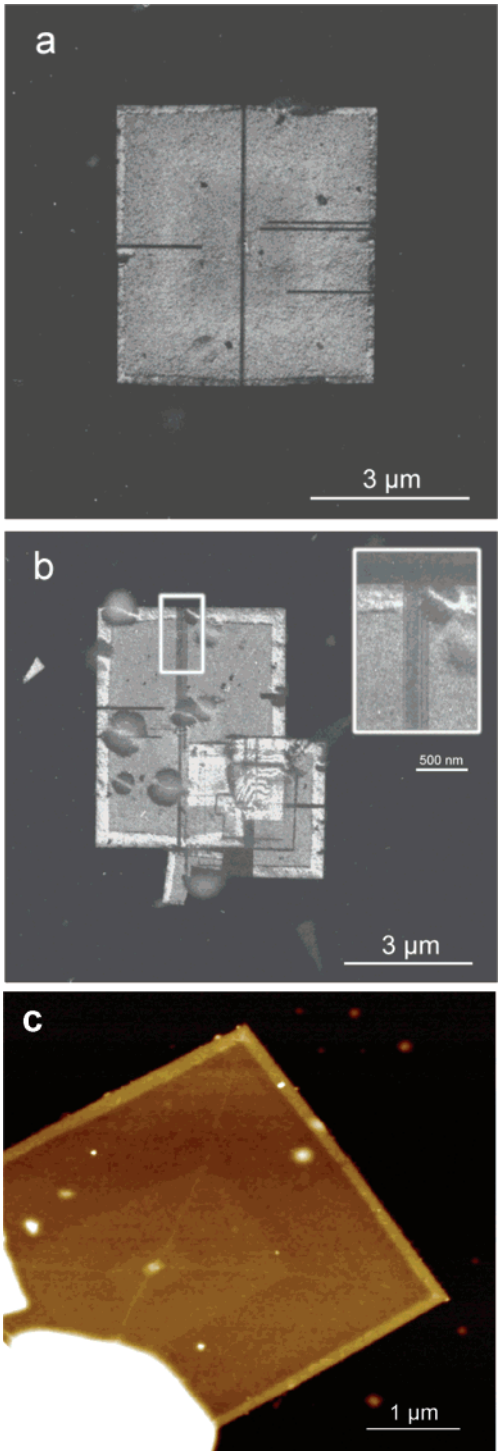

Figure 12. Single crystals of PVCH produced in squalane at 240 °C and imaged in dark field electron microscopy (a, b). Crystals shown have a rectangular shape, linked with the existence of a twin plane (part a) or of arrays (part b) of nearby twin planes in the initial seed. This (these) twin plane(s) induce a higher growth rate through fractional secondary nucleation. Growth twins are less frequent than for lower crystallization temperatures. Note the outer, thicker rim (brighter in this imaging mode) that may correspond to crystallization of a lower MW fraction of the polymer. (c) Similar crystals as examined by AFM. Note the thicker outer rim in the height image, and the central twin planes giving rise to the higher growth rate.

for PVCH, in the frame of crystal growth processes.

In the present investigation, twinning gives access to lateral spread, i.e., to a multimolecular feature of polymer crystallization. If each secondary nucleation and its associated lateral spread is considered as the building block of the crystal growth, i.e., as a single entity, the investigation tool must be some crystallographic feature that differentiates the resulting building block from its neighbors. Growth twins as formed in PVCH crystals are well adapted to the present investigation. The twinning by merohedry generates a "mild" perturbation since the orientation of the unit cell axes is maintained during further growth. Also, the lateral spread of a twinned domain is "homogeneous": only "twinned" stems can contribute to the twinned strip extension (deposition of an "untwinned" stem would create a vacancy half a stem wide in the growth strip). Twinning is therefore a marker that highlights a feature that, being no longer molecular, reaches a parameter of the crystallization process—the lateral spread after initial secondary nucleation—that has not been accessible so far.

Growth Processes, Twinning as Marker and Possible Further Developments. Whereas growth twins offer the possibility to determine the lateral spreads during single-crystal growth—or at least to access a meaningful sampling as mentioned in the Introduction—twinning is, inherently, a perturbation of conventional crystallization and implies an energy penalty. The different nucleation and growth processes schematized in Figure 2b may be ranked according to the associated interface energies involved. Using the conventional notations (a and l are the stem width and length, σ_e and σ the end and the lateral surface energies, and $\Delta\sigma$ is the energy penalty, i.e., the difference in lateral energy between the twinned and crystallographic packing), these energies are as follows.

Twinned secondary nucleation: $2al\sigma + al\,\Delta\sigma + 2a^2\sigma_e$.

Secondary nucleation: $2al\sigma + 2a^2\sigma_e$.

Fractional secondary nucleation: $al\,\sigma + (al\,\Delta\sigma/2) + 2a^2\sigma_e$.

Twinned lateral spread: $al\,\Delta\sigma + 2a^2\sigma_e$.

Lateral spread: $2a^2\sigma_e$.

The analysis of PVCH single crystals structure and growth patterns introduces three new processes. Twinned secondary nucleation and twinned lateral spread have higher energies than the corresponding untwinned processes. Fractional secondary nucleation arising from the existence of a jag in the growth front, has however a lower energy than secondary nucleation.

Evaluation of the impact of these different processes is necessary to validate the approach used in this investigation. This analysis uses the crystal growth processes observed at high T_cs, when the (presumably small) differences in energy become critical. The rate of twinned secondary nucleation decreases significantly at high T_c (240 °C). It even vanishes at higher temperatures: crystallization from the bulk (in thin films) produces crystals that are only twinned at the center, with no further appearance of twinned domains via growth twinning.[15] At the same time, untwinned crystals do grow at these high temperatures, indicating that secondary nucleation is still active. Therefore, the very high T_c range is not accessible with our approach. At lower temperatures, however, twinned secondary nucleation is frequent enough to generate sufficient domains and allow the sampling of lateral spreads.

The *rates* of lateral spread for both twinned and untwinned domains cannot be measured and thus compared. The technique only measures the *extent* of lateral spread, which depends mostly on the nucleation density. We assume that possible differences in these rates play a secondary role in the present analysis (we will return to this point later). Twinned lateral spread may undervalue the crystallographic lateral spread extent and the location of the fitting curves in Figures 10 and 11 be slightly shifted to the right, especially those corresponding to high T_c. However, the overall tendency and distribution with changing crystallization temperature may not be affected.

The density of twinned secondary nucleation is relatively low (at least at sufficiently high T_cs). Every twinned domain is the result of a single secondary nucleation event and its associated lateral growth that takes place initially in a *single* growth layer one nanometer thick. In a crystal 5 μm wide, this corresponds to four growth sectors made of 2500 growth layers each, with spans ranging from 0 (at the center) to 5 μm (outer edge). Since twinned nucleation amounts at best to several hundred in any one crystal, the probability for two twinned secondary nucleation events to take place next to each other and in the same growth layer is very remote (but of course increases at very low T_c). In essence, the lateral size of the twinned domains reflects merely the so-called "niche separation" between secondary nucleation sites, keeping in mind that neighbor domains are untwinned.

The impact of fractional secondary nucleation − nucleation at a jag of the growth face—is best revealed by the rectangular shape of some crystals grown at 240 °C and nucleated by a twinned seed (Figure 12), i.e., when growth associated with a twin plane can be differentiated from that of untwinned growth face. The impact on growth rates of fractional secondary nucleation was discussed and suspected, but not demonstrated, in our previous report on polysynthetic twins of PVCH.[5] Crystals produced at 240 °C illustrate most conspicuously that fractional secondary nucleation can become the most effective process when conventional secondary nucleation is no longer, or is less operative.

To summarize this section, growth twinning provides a marker that helps determine the extent of lateral spread of twinned secondary nucleation as also determined by the encounter with nearby untwinned lateral spread (cf. Figure 2b). As such, the measure corresponds more exactly to the "niche separation" between secondary nucleation sites. By implication, the density of secondary nucleation on the growth faces of crystals can be determined. The technique is however limited, at low T_cs by the high density of twinned domains and at high T_c by the fact that growth twins are no longer formed.

Despite these limitations, further developments may be considered, although they were not attempted in the frame of the present work. In the various expressions of the growth rate G feature one constant—the layer thickness b—and two variables—the rate of secondary nucleation i and either the extent L' or the rate of lateral spread g. Our results provide a means to measure the lateral spread L' and to infer a density of secondary nucleation on the growth face. Conversion to the secondary nucleation and lateral spread *rates* requires merely introducing time, or combining the present measurements with the overall growth rate G.

In the specific case of PVCH crystals grown from squalane solutions, measurement of growth rates are difficult due to the high temperatures involved. They have not yet been performed. The best approach would be to use a temperature jump technique inspired from the earlier works of Point et al.[2] In essence, the isothermal crystallization experiment is disrupted at two times separated by a known interval (e.g., 1 h) by a short excursion to a higher crystallization temperature. This excursion generates a small annulus of a thicker lamella. AFM imaging reveals the steps in the single crystals and thus the width of the annulus, i.e., allows a direct measurement of the growth rate during the excursion. Note however that the growth rates measured would most certainly be those of twinned (rather than untwinned) crystals, i.e., would be determined by "fractional" secondary nucleation rather than by "true" secondary nucleation and lateral spread—which actually would correspond to a more realistic picture of the growth process in, e.g., bulk PVCH.

Comparison with Existing Theories of Polymer Crystal Growth. Keeping in mind the underlying assumptions and limitations of growth twinning as a marker developed above, the information made accessible by the present investigation of PVCH single crystals need to be analyzed in the context of theories of polymer crystal growth. Several theories have been proposed over the years, with a recent renewed interest in this topic.[16] The most striking feature of this analysis is however the fact that all the phenomena reported here—some of which are new—can be rationalized in terms of the standard theory of nucleation and growth that has been in the literature for many years.[1,4,17] In essence, the concepts developed in the frame of these theories are immediately transposable to, e.g., fractional secondary nucleation that was not considered in the early theories.

Beyond the possibility to image individual secondary nucleation and lateral growth processes, several major features emerge indeed from the data collected during these studies: (i) the large variation of the lateral spread with crystallization temperature, (ii) the wide distribution of domain widths at a given T_c and its narrowing at lower crystallization temperatures, and (iii) the lateral spreads measured in the present investigation correspond quite well with earlier estimates.

The correspondence is at times even surprising. If we refer to Figure 5, the number of stems deposited on a growth face (in that case, of polyethylene) by lateral spread varies slowly at low T_c, then increases quickly in the so-called regime II and reaches values higher than 100 in regime I. This curve was suggested when no reliable measure of lateral spread was available.[8] Strikingly, the number of stems corresponding to one twin domain in PVCH crystals is in the same range: it varies from 35 to 60 (on average), and is therefore located in the heart of this curve. The overall feeling is that the T_c range covered in our experiments corresponds roughly to a so-called regime II, possibly even through the range of the upswing displayed by the curve.

Domain I may have been reached, at least for the growth of the outer, thicker rim visible in the crystals produced in the high T_c range. Indeed, the edge of the crystal is flat. This may mean that lateral spread fills in completely the growth face after the fractional secondary nucleation at the twin plane abutting at the growth face center. At the same time, however, formation of this rim is accompanied by frequent loss of the substrate cw or ccw orientation of the stems, which may suggest other, less "cooperative" nucleation and growth mechanisms, possibly associated with the lower molecular weight of the depositing material.

Domain III supposes or requires very high secondary nucleation densities that cannot be accessed by the present technique (resolution limit of the imaging technique and/or instability of narrow twinned domains, as discussed above). Its existence cannot therefore be established in the present investigation. However, as observed in the growth pattern of crystals produced at 240 °C, there is a much higher probability of lateral spread than of secondary nucleation and even, for that matter, of fractional secondary nucleation. It was shown that 23 stems are deposited before the next fractional secondary nucleation takes place on the same side of the twin plane and generates a new layer. This is consistent with the relative energies involved in the process. Higher secondary nucleation rates are of course observed at lower T_cs, which reduces the impact of lateral spread, but the energy penalty of secondary nucleation remains valid. The high density of secondary nucleation assumed to take place in regime III, essentially only three stems apart, appears

excessive since lateral spread should be more effective in filling small niches than additional secondary nucleation.

The present results also indicate that straightforward application of the standard nucleation and growth theory may be dangerous. For example, they indicate that it is risky to analyze growth rate data for any polymer without a prior and intimate knowledge of whatever processes may disturb the growth process. Point et al. has already warned about such possible difficulties,[2] and Armistead and Goldbeck-Wood provide a critical review on these topics.[17] The present investigation of PVCH crystals points at growth twins as a possible pitfall that modifies growth rates.

In a more general context, the very existence of growth regimes, although used extensively in this paper as an easy means to describe growth processes, appears to be only faintly supported by experimental evidence. As already indicated, growth regimes are, or should be, associated with differences in the impact of lateral spread (through the relative variations of secondary nucleation i and lateral growth g rates). However, the curve of the extent of lateral spread is continuous, and the frontiers between the different growth regimes are at best ill defined (Figure 5). The regime III−regime II boundary corresponds to a more or less "theoretical" boundary (1.5 stems deposited after secondary nucleation).[8] The boundary between regimes II and I is "established" only in the case of polyethylene, and moreover on a morphological criterion. Armistead and Hoffman[8] analyze indeed the experimental results of Toda[18] and suggest that the regime I to II transition is associated with a significant morphological change in the habit of the PE crystals. In regime II, the (110) faces of crystals are well developed, whereas they tend to become quite small at higher T_c (the experiments were conducted in poor solvents of PE, namely in higher alkohols). These authors thus conclude that the whole length of the (110) face at high temperature is covered by lateral growth (thus regime I) whereas at lower temperature, the larger size of the (110) faces results from multiple nucleation (thus regime II).[19]

The existence of growth regimes rests also on the analysis of growth rate data in terms of the by now familiar log G vs $1/T\Delta T$ plot that displays breaks in the curves with slopes in a ratio of 1 to 2.[8] The existence and location of these breaks depends however critically on the choice of the melting temperature T_m.

Finally, and as already pointed out earlier, regime II extends over nearly 2 orders of magnitude of the number of stems deposited by lateral spread (Figure 5). It might be necessary to evaluate if the growth schemes supposed to apply for regime II (multiple nucleation, including on the developing strip) can be considered as fulfilled over such a wide range of lateral spreads.

Beyond these more specific issues, the present investigation highlights the surface selectivity of the nucleation and growth processes as part of a global process of surface recognition. The nucleation rates are highly dependent on the topography of the growth face and matching between deposited stem and substrate: for example, fractional secondary nucleation takes advantage of a jag in the growth front. Twinned secondary nucleation corresponds to an acceptable, but poorer interaction of the depositing stem and the crystal face than untwinned secondary nucleation. Its rate is indeed reduced relative to the untwinned one, and it fades out at high T_c. This "topographic matching" taking place at the growth front has already been discussed from a structural standpoint in earlier papers dealing with crystal growth[20] and epitaxy,[21] but mostly from a "static" viewpoint. The present investigation provides similar, but more "dynamic" evidence through its impact on elementary crystallization processes.

Conclusion

Twinning by merohedry in PVCH crystals[5] is a mild perturbation that does not change the unit cell orientation and affects little the growth process, but generates domains that can be visualized by dark field imaging in electron microscopy. It has been used as a structural probe to determine two processes involved in crystal growth: lateral spread and secondary nucleation. With each (twinned) secondary nucleation event is associated a twinned lateral spread. The lateral size of the twinned domains thus helps measure the lateral spread extent associated with each (twinned) secondary nucleation on the growth face (or in other words the "niche separation"). With the proviso of inherent small energy penalties, twinned lateral spread is representative of the crystallographic lateral spread and, by inference, the density of secondary nucleation. Both quantities had eluded all experimental approaches.

Both the average lateral spread and its variation with temperature have been determined for PVCH single crystals grown in a wide temperature range (120−240 °C). The lateral spread increases and broadens at high temperatures, decreases and narrows at lower temperatures, ranging on average from ≈ 35 to 60 stems (each ≈ 1 nm wide), at 120 and 220 °C, respectively. The density of secondary nucleation thus ranges from 30 to 15 per micrometer in the growth layers. These observations, as well as more specific features uncovered in this investigation (e.g., increased growth rate associated with fractional secondary nucleation at abutting twin planes, or clusters of twin planes) are amenable to an analysis that uses the ingredients of the standard "nucleation and growth" scheme of polymer crystallization. It appears that the crystallization range explored in this investigation of solution grown PVCH crystals corresponds to the so-called polynucleation regime or regime II. The various growth mechanisms uncovered (twinned secondary nucleation, twinned lateral spread, fractional secondary nucleation) help build up a more complex crystal growth scheme (even for single crystals) than the standard "crystallographic" secondary nucleation and lateral spread considered so far in polymer crystallization. Moreover, they provide a unique and challenging experimental frame that should help assess the validity of current theories and modeling procedures used to analyze polymer crystal growth.

Acknowledgment. We thank Mr. C. Contal (Institut Charles Sadron, Strasbourg, France) for his help in the atomic force imaging part of this work.

Supporting Information Available: Text giving technical details on the high-resolution image acquisition and processing and figures showing further micrographs of twinned crystals produced at the various T_cs and not shown in this paper. This material is available free of charge via the Internet at http://pubs.acs.org.

References and Notes

(1) Hoffman, J. D.; Frolen, L. J.; Ross, G. S.; Lauritzen, J. I., Jr. *J. Res. Natl. Bur. Stand. Sect. A* **1975**, *79*, 671. Hoffman, J. D.; Davis, G. T.; Lauritzen, J. I. Jr. In *Treatise on Solid State Chemistry*; Hannay, N. B., Ed.; Plenum Press: New York, 1976; Vol. 3, pp 497−614.

(2) Point, J. J.; Colet, M. C.; Dosière, M. *J. Polym. Sci., Polym. Phys. Ed.* **1986**, *24*, 357. Point, J. J.; Damman, P.; Janimak, J. J. *Polymer* **1993**, *34*, 3771.

(3) Cheng, S. Z. D.; Lotz, B. *Polymer* **2005**, *46*, 8662.

(4) Hoffman, J. D.; Miller, R. L. *Macromolecules* **1989**, *22*, 3502.

CDV

(5) Alcazar, D.; Ruan, J.; Thierry, A.; Kawaguchi, A.; Lotz, B. *Macromolecules* **2006**, *39*, 1008.
(6) De Rosa, C.; Borriello, A. M.; Corradini, P. *Macromolecules* **1996**, *29*, 6323.
(7) Nishikawa, Y.; Murakami, S.; Kohjiya, S.; Kawaguchi, A. *Macromolecules* **1996**, *29*, 5558.
(8) Armistead, J. P.; Hoffman, J. D. *Macromolecules* **2002**, *35*, 3895−3913.
(9) Guttman, C. M.; DiMarzio, E. A. *J. Appl. Phys.* **1983**, *54*, 5541.
(10) Sanchez, I. C.; Di Marzio, E. A. *J. Chem. Phys.* **1971**, *55*, 893.
(11) Sadler, D. M.; Spells, S. J.; Keller, A.; Guenet, J. M. *Polym. Commun.* **1984**, *25*, 290.
(12) Wittmann J. C.; Lotz, B. *J. Polym. Sci., Polym. Phys. Ed.* **1985**, *23*, 205.
(13) Pradère, P.; Revol, J. F.; Manley, R. St. J. *Macromolecules* **1988**, *21*, 2747.
(14) Tsuji, M.; Okihara, T.; Tosaka, M.; Kawaguchi, A.; Katayama, K. *MSA Bull.* **1993**, *23*, 57; Tosaka, M.; Hamada, N.; Tsuji, M.; Kohjiya, S. *Macromolecules* **1997**, *30*, 6592. Tosaka, M.; Tsuji, M.; Cartier, L.; Lotz, B.; Kohjiya, S.; Ogawa, T.; Isoda, S.; Kobayashi, T. *Polymer* **1998**, *39*, 5273. Tosaka, M.; Tsuji, M.; Kohjiya, S.; Cartier, L.; Lotz, B. *Macromolecules* **1999**, *32*, 4905.
(15) Alcazar, D.; Ruan, J.; Thierry, A.; Lotz, B. *Macromolecules* **2006**, *39*, 2832.
(16) Strobl, G. *Eur. Phys. J. E: Soft Matter* **2000**, *3*, 165. Strobl, G. *Prog. Polym. Sci.* **2006**, *31*, 398. Olmsted, P. D.; Poon, W. C. K.; McLeish, T. C. B.; Terrill, N. J.; Ryan, A. J. *Phys. Rev. Lett.* **1998**, *81*, 373. Imai, M.; Kaji, K.; Kanaya, T. *Phys. Rev. Lett.* **1993**, *71*, 4162. Matsuba, G.; Kanaya, T.; Saito, M.; Kaji, K.; Nishida, K. *Phys. Rev. E* **2000**, *62*, R1497. Liu, L.; Muthukumar, M. *J. Chem. Phys.* **1998**, *109*, 2536. Muthukumar, M. *Philos. Trans. R. Soc. London A* **2003**, *361*, 538. See also a number of papers relating to this topic in volumes 180, 190 and 191 of *Adv. Polym. Sci.*, (**2005** and **2006**), "Interphases and Mesophases in Polymer Crystallisation", G. Allegra, Ed.
(17) Armitstead, K.; Goldbeck-Wood, G. *Adv. Polym. Sci.* **1992**, *100*, 221.
(18) Toda, A. *Faraday Discuss.* **1993**, *95*, 129. Toda, A. *Colloid Polym. Sci.* **1992**, *270*, 667.
(19) Mansfield, M. L. *Polymer* **1988**, *29*, 1755. Mansfield, M. L. *Polym. Commun.* **1990**, *31*, 283.
(20) Lotz, B. *Eur. Phys. J. E: Soft Matter* **2000**, *3*, 185.
(21) Lotz, B. *Adv. Polym. Sci.* **2005**, *180*, 17.

MA061697X